

Analysis of Neodymium-Doped Yttrium-Aluminum-Garnet Laser and Experimental Prospects for Cutting Micro-Thin Black Walnut Veneers in Industry

Bakary S. Doumbia,^{a,b,c} Chunmei Yang,^{a,b,*} Yan Ma,^a Ting Jiang,^{a,b} Xiang Li,^{a,b} and Wenji Yu^{b,d,*}

By structurally and practically analyzing the use of Nd: YAG laser for cutting black walnut veneer, this study considered practical and environmental concerns regarding the global warming protection measures. A numerical model of laser wood veneer cutting was based on the relation between process parameters and the material thickness. A pulsed Nd: YAG was used to cut black walnut veneer of 0.3 mm thickness under different machining conditions regarding laser power and cutting speed to study the cut kerf width. An analysis of variance was conducted to test the significance of machining parameters. The parameters studied were laser power, cutting speed, kerf width, cut surface, safety, and eco-friendliness. The results showed that the kerf width decreased significantly with increased cut speed and, inversely, by laser output power. An efficient cut with a narrow kerf, clean and smooth, with less burn, was possible at laser cutting speeds of 2.5, 5.0, and 5.5 mm/s with kerf widths of 0.544, 0.69, 0.62 mm, respectively. As multiple factors affect the micro-thin wood laser cutting process, finding the optimal process parameters is crucial for successful machining with no burn effect.

Keywords: Black walnut veneer; Cut quality; Eco-friendly; Kerf width; Micro-thin wood objects; Nanosecond Nd-YAG laser

Contact information: a: Forestry and Woodworking Machinery Engineering Technology Center, Northeast Forestry University, Harbin 150040, China; b: Northeast Forestry University, College of Mechanical and Electrical Engineering, Harbin, 150040, China; c: University of Science Technical and Technology of Bamako (USTTB), Faculty of Sciences and Technology (FAST), Bamako 423, Mali; d: Research Institute of Wood Industry, Chinese Academy of Forestry, Beijing, 100091, China;

* Corresponding authors: yuwenji@caf.ac.cn; ycmnefu@126.com

INTRODUCTION

Rapid prototyping technologies (RPTs) have been applied in various sectors, including the manufacturing of metallic and non-metal materials, which require lasers. Object laser cutting is one of the most applied techniques with numerous kinds of lasers. The most commonly used, conventional laser techniques are carbon dioxide (CO₂), fiber/disk, neodymium-doped: yttrium-aluminum-garnet (Nd: YAG), and direct diode lasers (Choudhury and Shirley 2010; Tahir *et al.* 2012a; Pocorni *et al.* 2017). Some of these lasers are physically identical but utterly different in terms of physical properties, components, operating modes and processes, and the range of applicability in terms of materials. These lasers and their derivatives have become more competitive regarding the multiple advantages owned and the service quality that they may provide. The selection of laser cutting technique depends on the desired object and on the precision and flexibility of cutting the contour (laser output power and cutting speed), cut edge quality, small heat-

affected zone (HAZ), and the potential for process automatization (Powell and Kaplan 2004). For efficiency and versatility purposes, a gas or liquid is often used in laser cutting to remove debris from the cut surface.

The Nd: YAG solid-state laser is used for high precision and micro-processing applications. While it is practically suited for metallic materials application, its application with organic materials (nonmetallic) has grown significantly. As a result, a low-power 500 W Nd: YAG laser with 20 mm/s of cut speed has been used to cut nylon seat belts (Tahir *et al.* 2012a). The laser beam cut and sealed the workpiece with a minimum flare without any burr observed on the edges. However, the process freed some noxious gases that are dangerous for user health and environmentally harmful. A 275 W Nd: YAG laser of 254 mm of focal length, with a coaxial gas flow, has been used to cleanly cut 114 mm thick of rubber foam at a laser speed of 16.6 mm/s without any sign of burn reported (Tahir *et al.* 2012a). As reported in Peters and Marshall (1975), a 1 kW Nd: YAG laser was used to cut the plastic part. In sum, the Nd: YAG laser is an excellent technique for cutting speed, cleanliness, and overall process time consumption.

In pulsed mode, the laser works in pulses, generating short pulses, each with high laser output power. The pulse duration and pause duration alternate at short intervals and produce pulses with maximum output. The shortest-duration laser created to this point produced pulses of six-femtoseconds duration, a time that corresponds to the only three optical cycles (Fork *et al.* 1989). The more energetic pulsed mode is suited for materials processing applications (Powell 1998). Low-powered lasers mainly use the process for specific applications, resulting in small contours or embellishment slats with a width smaller than the material thickness. Pulsed lasers are widely applied for material processing, namely, in fine cutting, welding, and hole drilling (Olsen and Alting 1995). They are flexible equipment for scientists and engineers that have achieved a vital function in current optical physics (Zhu and Hall 1997). Notably, the primary pulsed laser was invented by T. H. Maiman (Maiman 1960). Due to their high peak power, pulsed lasers have helped researchers to view and study outcomes that scale nonlinearly with growing the strength of the optical region. These kinds of lasers can be highly cost-effective. They have been shown to be especially useful in studying transient phenomena that occur in periods as brief as femtoseconds or so long as milliseconds or beyond (Zhu and Hall 1997). Accordingly, pulsed lasers have been utilized for a wide range of products and items for decades and have become an indispensable part of advanced manufacturing (AM) technology (Trumpf 2007). As a result, for current use, a pulsed Nd: YAG solid-state laser was used to investigate the cut surface quality of different types of wood materials regarding the impact of the laser energy, feed rate, and kerf depth, showing excellent results depending on the laser pulse frequency, power, and feed rate (Xinbo *et al.* 2016). Yang *et al.* (2018) used pulsed Nd: YAG laser with and without water jet-assisted to cut Korean pinewood with a thickness of 2 mm. The study showed significant machining results depending on the influence of the cutting speed, laser power on cut surface quality, namely the kerf of the cut. Yang *et al.* (2017) proposed the nanosecond laser processing theory of micronized wood fibers, demonstrated the possibility of cutting micronized wood fibers along the grain, and concluded that the use of a nanosecond laser ensures accuracy in the micron range.

Wood is a renewable, biodegradable material with a wide range of applications, from furniture to architecture. Wood veneer is a thin layer of woodcut mainly used for interior decoration applications. It is ideal for residential projects, hotel projects, offices, *etc.* Moreover, veneer is processed to create various products such as veneer parquet,

flexible veneer sheets, veneer boards, and veneer wallpaper. In manufacturing sectors, laser applications provide new theories and have made things comfortable and straightforward (Yang *et al.* 2017). Consequently, the unique beam characterizations of Nd: YAG lasers promote safety and flexibility compared with other lasers. However, in terms of its application for wood veneer parts machining, there is an absence of detailed investigations regarding the laser structure, process analysis, and applicability.

This paper examines Nd: YAG laser cutting of black walnut veneers for use in industry. The findings provide an insight for the structural and practical use of Nd: YAG laser cutting of micro-thin wood objects regarding laser safety and eco-friendliness.

Structure and Analysis of Neodymium-Doped: Yttrium-Aluminum-Garnet (Nd: Yag) Laser

Yttrium aluminum garnet (YAG), a single synthetic crystal of $Y_3Al_5O_{12}$ doped with a low percentage of the rare-earth element neodymium (Nd^{3+} ion), which constitutes the active laser medium (Nd: YAG laser); it transmits infrared laser radiation at the wavelength of $1.064 \mu m$. The ion Nd^{3+} hosts the YAG carrying out the lasing action.

Construction and Principle

The broadband optical radiation from the pulsed krypton flash, continuous wave (CW) lamp, or laser diode coupled into the crystal excites the active medium (Nd^{3+} ions) to the high energy levels (Wandera 2006). During the passage from the metastable state to the ground state, the laser beam emits a wavelength of $1.064 \mu m$. YAG crystal acts as a positive lens when pumped because of the high temperature at the center as the cooling water is in contact only with the outer surface. This thermal lensing of the rod increases while increasing the pump power (Almeida *et al.* 2018). An elliptical cylindrical reflector keeps the crystal (laser rod) and the flash lamp at its focus. Both ends of the laser rod are polished. It is optically active in the resonator. This optical resonator is constituted of two mirrors M_1 and M_2 , respectively, highly and partially reflective (Fig. 1). The optical characteristic variation depends on the laser parameters, which will affect the laser output power.

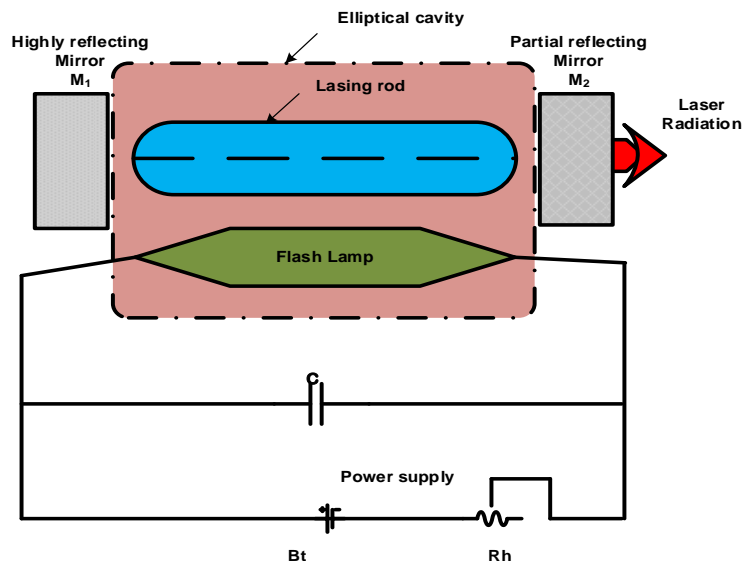


Fig. 1. Solid-state Nd: YAG laser construction mode

Nd: YAG is a four-level laser. Figure 2 displays the simplified four-level energy diagram of ions neodymium (Nd^{3+}). Once the krypton flash lamp is switched on, as shown in Fig. 1, the atoms of Nd^{3+} are pumped from the ground state energy level (E_0) to the upper states, E_3 and E_4 , constituting the crucial levels of the pump bands by absorption of the radiation of $0.73 \mu\text{m}$ and $0.80 \mu\text{m}$, respectively, for E_3 and E_4 (Svelto 2010). From E_3 and E_4 , atoms of Nd^{3+} transit to the energy state-level E_2 (metastable-state) by the non-radiative transition. The excited Nd^{3+} ions stay about $230 \mu\text{s}$ in E_2 , allowing a transition to energy state-level E_1 (Shabbusharma 2020). During this transition from E_2 and E_1 , radiation of $1.06 \mu\text{m}$ of wavelength is emitted. This photon ($\lambda = 1.06 \mu\text{m}$), while stimulating the transition, oscillates between the two mirrors M_2 and M_1 . Thus, through the partial reflecting mirror M_2 , a coherent output beam of the laser is obtained, as shown in Fig. 1. The population of ions Nd^{3+} on E_1 state is lower than that on state E_2 , so the population inversion is achieved (Shabbusharma 2020). The ions Nd^{3+} in the energy state E_1 (approx. 0.25 eV) quickly jump to ground state energy level E_0 under non-radiative transition (Svelto 2010; Shabbusharma 2020).

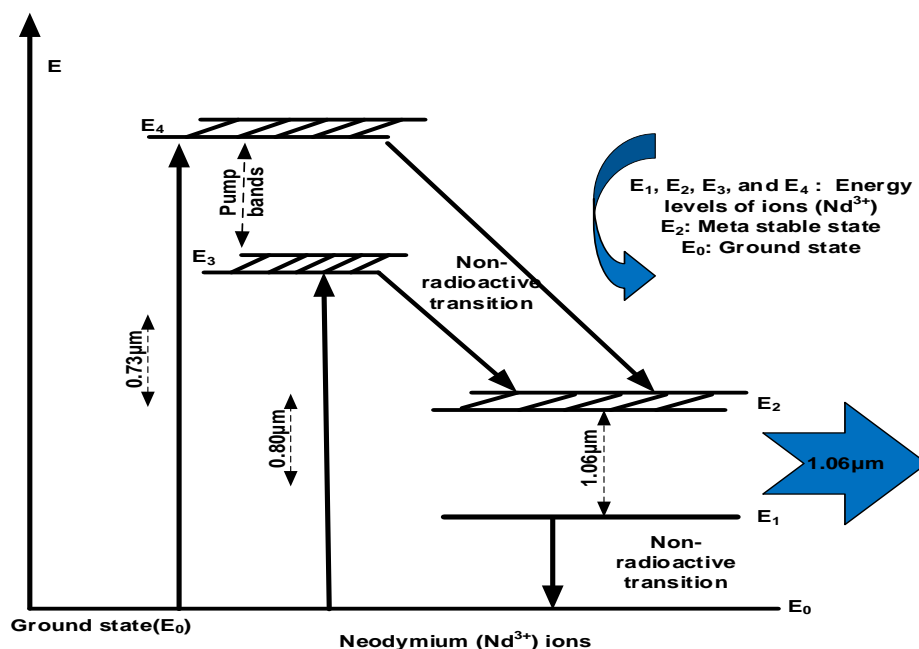


Fig. 2. Simplified energy state diagram and principle of Nd: YAG laser

Operating modes and processes

In pulsed mode, the flash lamps are explicitly designed for the typical repetitive high-peak-current electrical pulses to create the laser pulses (Borges 2008). The flash lamps have unique design features to improve their reliability and life regarding the high peak currents in the lamp during a pulse (Wandera 2006). Therefore, they can withstand the higher delivered average power. On the other hand, operating in the continuous mode (CW) requires much higher pumping energy because of lower photon flux in the laser. The cooling optimized for the high-power operation, and the high-pressure spikes of pulsing lights source, which is absent with CW lamps. The lamp jacket walls are thin, and the electrode size increases for better cooling (Wandera 2006). The electrodes are formed for repeatable arc production. Simultaneously, the mass and placement of the conductors are optimized for thermal stresses, whereas the metal electrode seals to the swallowed glass. The Nd: YAG laser operating setup on the object is schematized in Fig. 3.

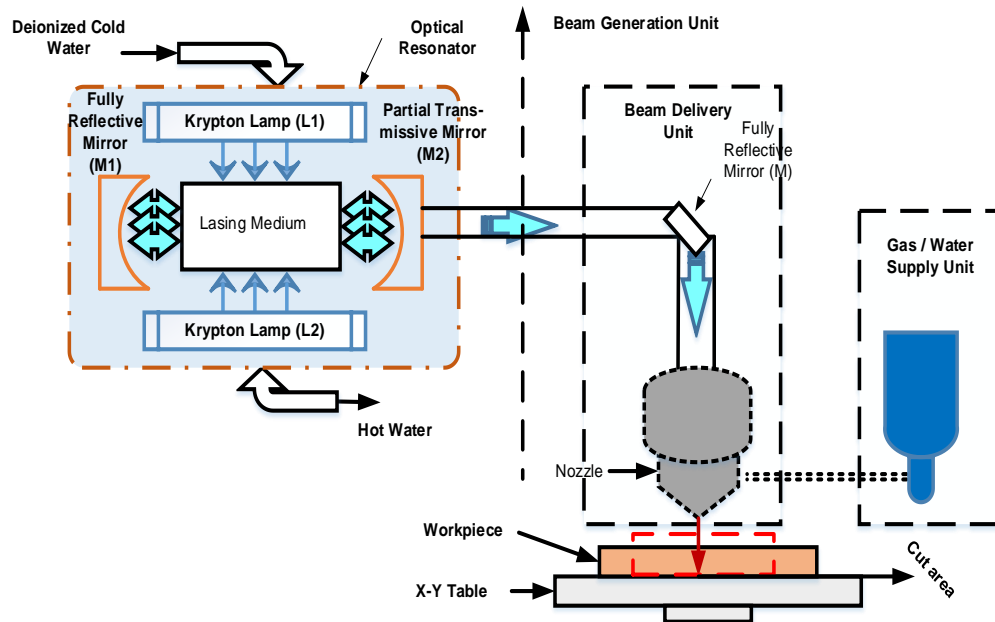


Fig. 3. Nd: YAG experimental laser setup

Nd: YAG Laser for Industrial Laser Cutting Applications

In advanced manufacturing (AM), the lasers with high beam quality and high power are more appropriate for cutting applications. Consequently, Nd: YAG laser technology is suited, straightforward, and overwhelmingly used high-power solid-state laser for high precision and micro-processing applications (Schuocker 1989; Guillas *et al.* 1990; Kalokasidis *et al.* 2013). However, the laser beam is quantitatively responsible for predicting suited types of materials for applications. This laser is available for application with an output power capability of up to 4,500 W (Senthilkumar *et al.* 2016). Nd: YAG lasers emit in the near-infrared at a wavelength of 1.06 μm . This wavelength is suited for overwhelming types of materials with less restriction. As a result, it is applied to a wide range of materials, including metallic and nonmetallic (Leone *et al.* 2009; Tahir *et al.* 2012a; Sharma and Yadava 2013; Gautam and Pandey 2018; Sharma and Yadava 2018). The YAG laser equipment is suited for machining complex geometries in general and, in particular, reflective items (Sharma and Yadava 2018). YAG is one of the sought-after laser machines for applications in sophisticated fields and susceptible objects.

For cutting nonmetallic objects

In terms of cutting items, Nd: YAG laser processes differently with different kinds of materials. Notably, most organic materials faintly absorb the YAG laser beam. However, it is practically efficient for operating with a certain number of nonmetallic materials, namely plastics, wood, rubber, and acrylic. Consequently, the use of Nd: YAG laser for cutting plastics and wooden items have recently gradually increased. As a result, numerous investigations have been reported using low-powered Nd: YAG lasers to cutting nonmetallic materials. A 1 kW Nd: YAG laser was used to cut reinforced plastic with the mold parts and compared with other techniques, such as water jet cutting, milling, punching, cutting traditional knife, and hot ultrasonic blade (Gong 2014). The study shows that the Nd: YAG laser cutting is faster and cleaner, and with a minimum time of process

than other techniques. A 560 W Nd: YAG laser was used to remove the ceramic material at a rate of 5.3 mm³/s (Sharma and Yadava 2018). A pulsed Nd: YAG solid-state laser was used to investigate the cutting quality of different types of wood sheets regarding the impact of the laser energy, feed rate, and kerf depth (Xinbo *et al.* 2016). The study found excellent results depending on the laser pulse frequency, power, and feed rate. Yang *et al.* (2018) used a pulsed Nd: YAG laser with and without water jet-assisted to cut Korean pinewood (*Pinus koraiensis*) with a thickness of 2 mm. In terms of the cut kerf, the study shows the increase with the increase of laser power and then the decrease with the increase of laser cutting speed.

EXPERIMENTAL

Materials and Equipment

This study analyzed the use of Nd: YAG laser laminated object manufacturing (LOM) based technology for micro-thin wood products prototyping in the industry. The system contained a solid-state laser, (Nd: YAG) laser, JDW3-250 laser power supply (Beijing, China). The Nd: YAG laser had a focal length of 15 cm and a spot diameter of 1 mm. The overall equipment is a mounting system with a calibration platform (Fig. 4(c)). A commercial black walnut veneer of 0.3 mm thick with 10% moisture content was used as the proceeded material. This workpiece was clamped on the lifting platform, as shown in Fig. 4(b). The system was cooled at 600 W by a PH-LW06-BLP laser cooling system (Shenzhen, China).

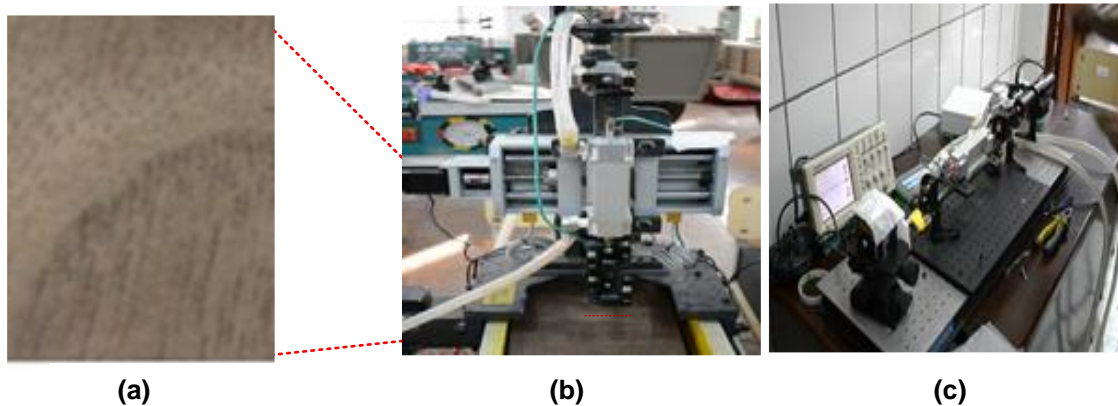


Fig. 4. Material and equipment for pulsed Nd: YAG laser experimental test. (a) Black walnut, (b) Nd: YAG laser system, (c) Laser calibration.

Process Methods

The nanosecond Nd: YAG was tested for cutting black walnut veneer through numerical and experimental analyses regarding parameters affecting the efficient machining with minimum burning effect. The veneer workpiece was laser cut at different cutting speeds corresponding to a laser output power. The cut surface quality and geometry related to the kerf width was investigated through measurement and microscopic observation. An analysis of variance was conducted to elucidate the relation between the laser cutting speed and the kerf width at specific laser output power. The average laser power and cutting speed were independent variables. The dependent variable under

investigation was the kerf width; additionally, non-numerical factors such as laser safety and eco-friendliness were considered.

Experimental process

A pre-experiment was conducted to calibrate the laser. An atomic gas type laser (helium-neon; He-Ne) with a focal length of 15 cm was used for laser calibration, as shown in Fig. 4(c). The measured focal length was 15.3 cm after calibration. The cut head of the Nd: YAG laser was mounted with the equipment by adjusting the working table for a chosen distance. Regarding the cut geometry, a plan interpolation allowed full movement along the workpiece at a planned position. Considering the black walnut veneer fiber structure, and additionally for an accurate, straightforward, and efficient cut results in terms of kerf width, a linear vertical laser-cut of the wood veneer was adopted. Table 1 depicts the laser parameters and characteristics. The black walnut laser-cut was performed according to two machining conditions related to laser output power and cutting speed. The cut area was blown using compressed air flow (see Fig. 4(b)). An optical microscope was used for visualizing, calculating the kerf width, and for cut surface micrographic analysis.

Table 1. Nd: YAG Laser Parameters

Pulse Width (μ s)	Pulse Frequency (Hz)	Pulse Voltage (V)	Pulse Energy (m.J)
200	1	300 to 800	10.8 to 489
200	5	300 to 800	16.4 to 578
200	10	300 to 800	18.4 to 602

Numerical process

During Nd: YAG micro-thin wood laser cutting process, as schematized in Fig. 3, numerous parameters were considered in terms of cutting quality, including the type of wood material, texture, thickness, water content, laser output power, cutting speed, *etc.* Due to the invariance of black walnut veneer thickness and its water content, the influence of laser power and cutting speed on cutting quality, namely the cut kerf, were studied. Depending on the laser power density, the cut can be efficient or not producing irradiation to cut through the workpiece. Thus, if the laser power density of the irradiation is enough, the material thermal decomposition is rapid, resulting in less heat transfer on the outside of the cutting area. Consequently, the cutting surface is slightly dark but presenting remarkable cutting quality. However, if the laser power density of laser radiation is insufficient, the workpiece may not cut thoroughly, and the material ignition point is reached, provoking slag and burning, which leads to a carbonized cut surface with a sizeable cut geometry.

Equations

As reported previously (Zhou and Mahdavian 2004; Xie *et al.* 2008), the mathematical model of Nd: YAG micro-thin wood laser cutting can be deduced as follows. During the process, the laser beam is focused on the surface of the workpiece with a radius of R . The cut depth occurs at the center $1/e^2$ of the focused radius, as shown in Fig. 5. Because the cut depth fall to the center $1/e^2$ of the focused radius, so the energy source distributed along the central line of the laser beam-moving trajectory is solely considered. Therefore, Eq. 1 expresses the balanced equation of energy conservation.

$$E_i = E_V + E_{Loss} \quad (1)$$

where E_i is the laser input energy (kJ), E_v is the energy required to cut the black walnut part (kJ), E_{Loss} is the energy loss (kJ), which has been ignored in this study.

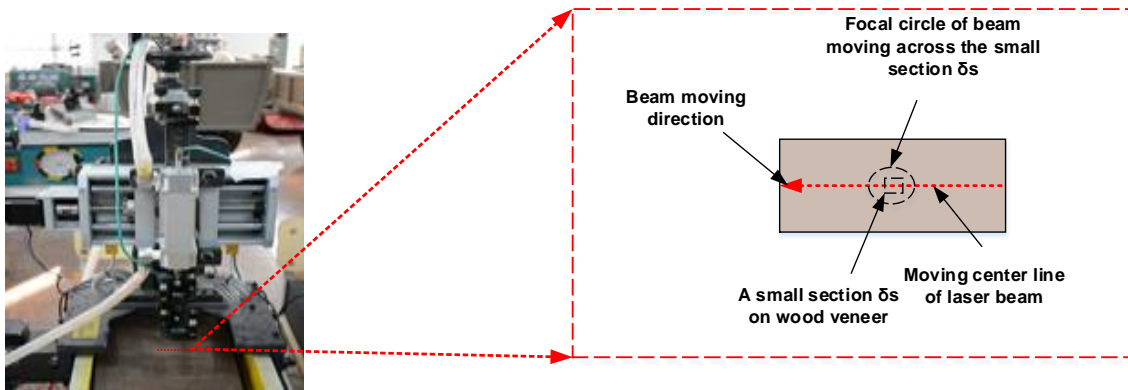


Fig. 5. Laser beam focal point on black walnut veneer.

Considering transverse electromagnetic mode (TEM00), which is suited and used by most industrial laser cutting processes (Zhou and Mahdavian 2004), Eq. 2 expresses the laser intensity distribution following TEM00,

$$I = \frac{AP_L}{\pi R^2} \exp\left(-\frac{X^2+Y^2}{R^2}\right) \quad (2)$$

where A is the laser absorption rate of the material (absorptivity); P_L is the laser peak power. R is the laser beam radius, denoting the center's distance to the point where the laser intensity value falls to $1/e^2$.

For pulsed Nd: YAG cutting of black walnut, the cut depth D (mm) for a small section $\delta S = \delta X \cdot \delta Y$ in the workpiece is expressed by Eq. 3 (Zhou and Mahdavian 2004; Yang *et al.* 2019),

$$D = \frac{A}{QR\sqrt{\pi}} \times \frac{P_L}{\vartheta} \quad (3)$$

where $Q = \rho[C_p(T_m - T_a) + L_v]$, which is related to the workpiece material. The variable ρ is the material density (kg/m^3), C_p is the specific heat capacity ($\text{J}/(\text{kg}\cdot^\circ\text{C})$), T_m is the melting temperature ($^\circ\text{C}$), T_a is the ambient temperature ($^\circ\text{C}$), and L_v is the latent heat of vaporization (J/kg), and ϑ is the laser cutting speed (mm/s).

The laser cutting speed ϑ and power P_L , and the material properties mainly affect the laser-cut depth. Consequently, the cut depth D is proportional to the laser power and inversely proportional to the laser cutting speed. Because P_L and ϑ are selected to cut through the micro-thin wood workpiece, the cut depth D can be assimilated to the thickness of the black walnut veneer (Yang *et al.* 2019).

RESULTS AND DISCUSSION

Results

Measurements

Considering the thickness of the black walnut of D (0.3 mm), as expressed in Eq.3, Table 2 depicts the characteristics of the black walnut veneer material.

Table 2. Properties and Values of Black Walnut Veneer

Properties	Value & Unit
Heat capacity (C_p)	$1.72 \cdot 10^3 \text{ J}/(\text{kg} \cdot ^\circ\text{C})$.
Average density (ρ)	$640 \text{ kg}/\text{m}^3$.
Melting temperature (T_m)	$500 \text{ }^\circ\text{C}$
Latent heat of vaporization (L_V)	$300.10^3 \text{ J}/\text{kg}$

The laser pulse width and focal radius are respectively ($t = 200 \mu\text{s}$, $R = 0.5 \text{ mm}$), with an absorptivity ($A = 0.5$). The ambient temperature (T_a) was selected as $25 \text{ }^\circ\text{C}$. Therefore, through calculation, $Q = 7.149 \cdot 10^8 \text{ J}$. Therefore, from Eq. 3, Eq. 4 deduces laser cutting as a function of peak power,

$$\vartheta = \frac{P_L}{380.1} \tag{4}$$

where P_L (W) denotes the average laser power, which is a function of laser single-pulse energy E (J) and the pulse frequency f (Hz) expressed by Eq. 5.

$$P_L = E \times f \tag{5}$$

As a result, Table 3 reports the numerical values of the cutting speed function of laser power. The discharge voltage had a noticeable impact on laser pulse energy and cutting speed. Consequently, the increase of laser discharge voltage resulted in higher average power, increasing laser cutting speed at a constant pulse frequency.

Table 3. Numerical Values of Laser Cutting Speed (Yang *et al.* 2019)

Discharge Voltage (V)	Single-pulse energy (m.J)	Pulse Frequency (Hz)	The Cutting Speed (mm/s)
300	18.4	10	0.484
400	96.5	10	2.538
500	198.2	10	5.214
600	317.4	10	8.35
700	468.8	10	12.334
800	602.3	10	15.846

Figure 6 depicts the variation between the three variables pulse voltage (V), pulse energy (m.J), and laser cutting speed (mm/s).

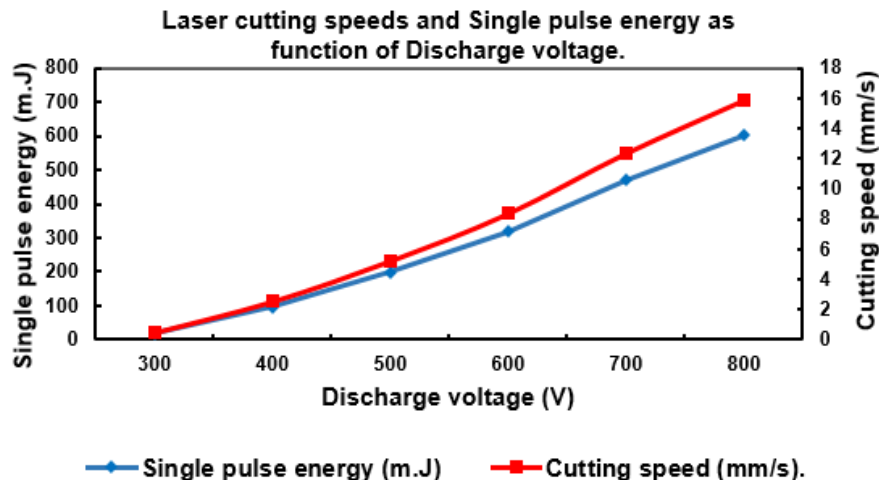


Fig. 6. Laser cutting speed and the pulse energy variation according to the discharge voltage

Experimental

Regarding the data in Table 3, two machining conditions were established randomly to carry out the black walnut veneer Nd: YAG laser-cutting test. These two conditions, S₁ and S₂, are shown in Table 4.

Table 4. Black Walnut Veneer Laser Cutting Conditions

Test condition	Pulse Voltage (V)	Pulse Energy (m.J)	Pulse Frequency (Hz)	Cutting Speed (mm/s)
S ₁	400	96.5	10	3.0, 2.5, 2.0, 1.5, 1.0, 0.5
S ₂	500	198.2	10	5.5, 5.0, 4.5, 4.0, 3.5, 3.0

As a result, Figs. 7 and 8 depict the cut surface at different laser cutting speeds under S₁ and S₂. Figure 7 shows cut under condition S₁ at different cutting speeds, namely of 0.5 mm/s, 1.0 mm/s, 1.5 mm/s, 2.0 mm/s, 2.5 mm/s, and 3.0 mm/. Figure 8 illustrates the result under condition S₂ with corresponding laser cutting speed of 3.0 mm/s, 3.5 mm/s, 4.0 mm/s, 4.5 mm/s, 5.0 mm/s, and 5.5 mm/s (Yang *et al.* 2019).

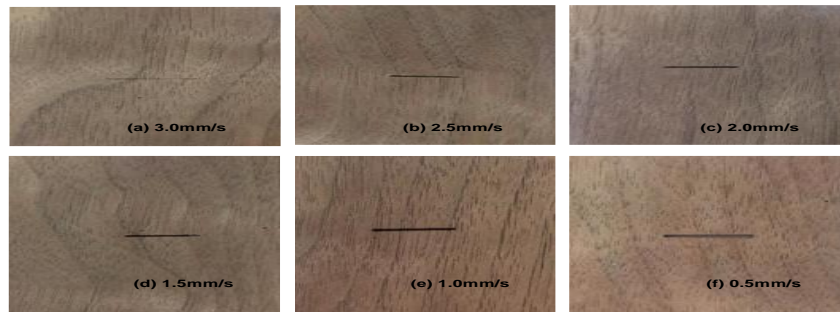


Fig. 7. Black walnut veneer cut surfaces at different laser cutting speeds under the machining condition of S₁

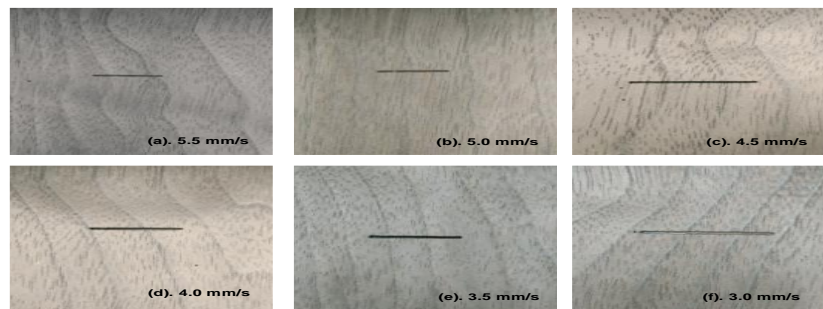


Fig. 8. Black walnut veneer cut surfaces at different laser cutting speeds under the machining condition of S₂

Considering the laser cutting speed under different machining conditions S₁ and S₂ as depicted in Table 4, and for each selected value, five (05) repetitive measurements of the kerf width along the cut line were reported. For each five-measurement group at corresponding laser cutting speed, the kerf width's average value is considered. The data are reported in Table 5 and 6 for S₁ and S₂, respectively. For S₁, the kerf width at the laser cutting speed of 3 mm/s was not considered for further analysis.

Table 5. Kerf Width of the Black Walnut under S₁

Laser Cutting Speed (mm/s)	Kerf Width (mm)
0.5	1.209
1	0.908
1.5	0.850
2	0.653
2.5	0.544

Table 6. Kerf Width of the Black Walnut veneer under S₂

Cutting Speed (mm/s)	Kerf Width (mm)
3.0	1.35
3.5	1.16
4.0	1.01
4.5	0.78
5.0	0.69
5.5	0.62

Figure 9 shows the graph of the black walnut veneer kerf width as a function of laser cutting speed. Similarly, as reported in Table 6, the relationship between the black walnut veneer kerf width and laser cutting speed under S₂ is shown in Fig. 10.

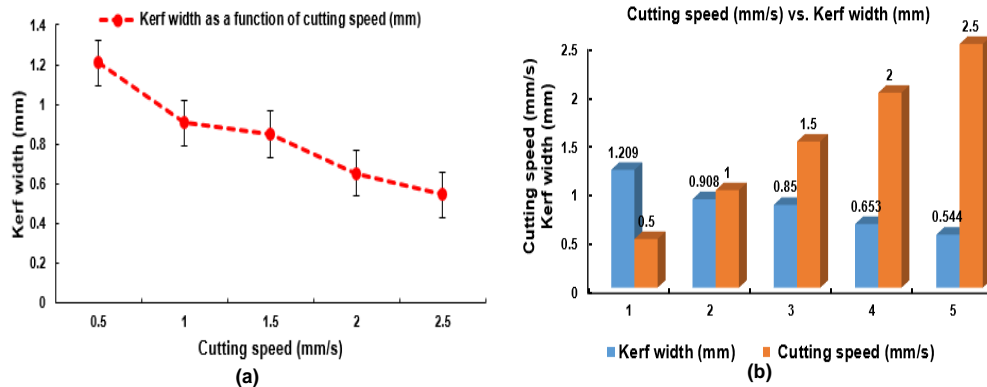


Fig. 9. The relation between laser cutting speed and the kerf width under S₁. (a) Kerf width as a function of Cutting speed, (b) Histogram of the Cutting speed vs. Kerf width

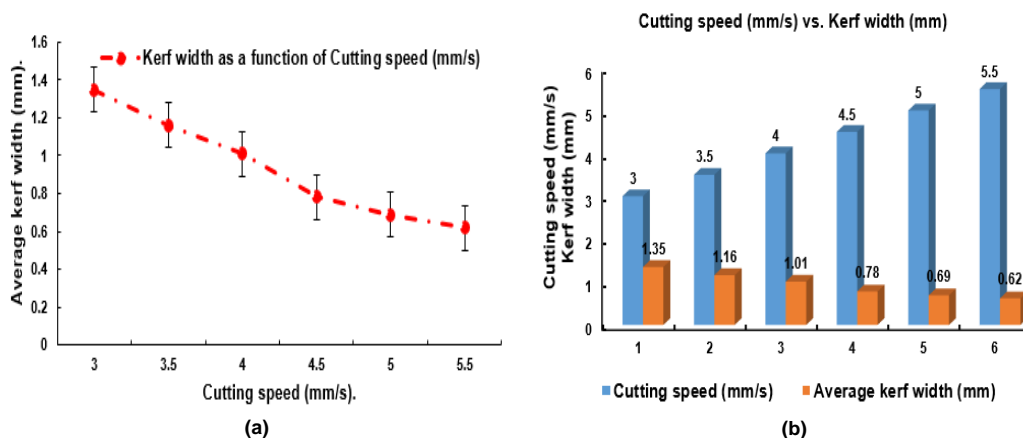


Fig. 110. The relation between laser cutting speed and the kerf width under S₂. (a) Kerf width as a function of laser cutting speed, (b) Histogram of the cutting speed vs. Kerf width

Discussion

Figures 9 and 10 show a noticeable influence of the laser cutting speed on the kerf width. Indeed, from both conditions (S_1) and (S_2), the kerf width decreased with the increase of the laser cutting speed and *vice-versa*. Moreover, considering S_1 and S_2 , One-way ANOVA single factor of laser cutting speed related to the kerf width data is reported in Table 7 and 8 for S_1 and S_2 , respectively.

Table 7. ANOVA of Kerf Width under S_1

Source of Variation	SS	df	MS	F	P-value	F crit
Between Groups	1.317398	4	0.329349	101.7453	5.35E-13	2.866081
Within Groups	0.06474	20	0.003237			
Total	1.382138	24				

Table 8. ANOVA of Kerf Width under S_2

Source of Variation	SS	df	MS	F	P-value	F crit
Between Groups	2.033387	5	0.406677	87.55163	1.31E-14	2.620654
Within Groups	0.11148	24	0.004645			
Total	2.144867	29				

In Table 7, considering the machining condition (S_1), in terms of the difference between the kerf widths group at different laser cutting speeds, the P-value (5.35E-13) was much below α (0.05). Besides, the F (101.7453) was much greater than the F-critical (2.8660814). Likewise, considering the condition (S_2), in Table 8, the P-value (1.31E-14) was far below α (0.05); also, the F (87.5516) was far greater than the F-critical (2.620654).

For both conditions S_1 and S_2 , there was a significant difference between the kerf widths at different laser cutting speeds under constant output power. In other words, the black walnut veneer laser cutting speed significantly influenced the cut kerf width.

Micro-morphology of black walnut veneer cut surface

Considering the laser cutting speed under machining conditions as reported in Table 4, while using an optical microscope, the black walnut cut surfaces were visualized. Figure 11 shows the micrograph of the cut surface of the black walnut veneer workpiece at different optimal laser cutting speed underneath S_1 and S_2 , respectively.

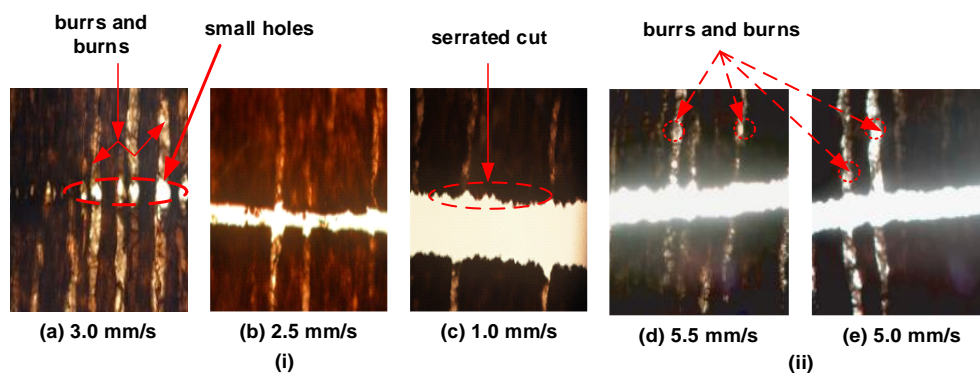


Fig. 211. Micrograph of the cut surface at different laser cutting speeds. (i) Laser output power condition of 400V of pulse voltage, single pulse energy of 96.5mJ, pulse frequency of 10Hz (S_1); (ii) Laser output power condition of 500 V of pulse voltage, single pulse energy of 198.2 mJ, pulse frequency of 10 Hz (S_2).

Figure 11(i) presents the micrograph of the walnut veneer cut surface under the condition S_1 at three different laser cutting speeds, namely 3.0 mm/s, 2.5 mm/s, and 1.0 mm/s, respectively for (a), (b), and (c). Figure 11(ii) corresponds to condition S_2 at laser cutting speed of 5.5 mm/s and 5.0 mm/s, respectively, for (d) and (e).

As shown in Fig. 11, the kerf width increased with the decreased laser cutting speed and *vice-versa* at selected laser power in both S_1 and S_2 . In Fig. 11(i).(a), when selecting the cutting speed of 3.0 mm/s, the laser failed to cut properly through the black walnut veneer while making a series of holes on its surface with noticeable burrs solely and burn effects. This may be due to the fast-cut speed considering the laser pulse energy, causing the black walnut veneer dark surface. In Fig. 11(i).(b), at laser cutting of 2.5 mm/s, the kerf width of 0.5438 mm was comparatively small, giving a cut geometry relatively smooth, clean with minimal burns, and less carbonization on the black walnut veneer surface. Comparatively, for the laser cutting speed of 1.0 mm/s in Fig.11(i).(c), the kerf width of 0.9084 mm is about twice that of 2.5 mm/s in Fig. 11(i).(b), providing serrated cut geometry with a continuous dark spot covering the surface. In Fig. 11(ii).(d), (e), respectively, for laser cutting speed of 5.5 mm/s and 5.0 mm/s, there is a slight variation on the kerf width, namely 0.622 mm and 0.688 mm, resulting in smooth cut areas but with noticeable burrs and burn effects, carbonized with continuous dark on veneer surfaces.

The optimal laser cutting speeds with remarkable cut results in terms of cut kerf width, namely 2.5 mm/s, 5.0, and 5.5 mm/s respectively for S_1 and S_2 , were numerically predicted, as shown in Table 3. Indeed, in Table 3, for condition S_1 the laser cutting speed is 2.538 mm/s. For condition S_2 , 5.214 mm/s is noticeable, approximately the average value of 5.5 mm/s and 5.0 mm/s, as shown in Fig. 11.

Accordingly, for a selected set up with the right parameter combinations, the Nd: YAG laser can perform to a smaller thermal load, narrow kerf width, and small HAZ (Gong 2014). Because the HAZ and the kerf width depend on the pulse energy, the use of high pulse energy at a short time leads to a decrease of the HAZ and the kerf width (Chien and Gupta 2005). Consequently, pulsed Nd: YAG was efficiently used to cut the CFRP plate of 1 mm of thickness at a laser cutting speed of about 11 mm/s (Leone *et al.* 2009). The Nd: YAG laser focus on a smaller spot diameter with higher power density leads to efficient machinability in terms of smaller kerf width and less thermal distortion; in other words, the heat-affected zone (HAZ).

Safety and eco-friendliness of Nd: YAG laser

The Nd: YAG laser for cutting black walnut veneer in particular, and in general for micro-thin wood applications, is a versatile technique. The YAG solid-state laser, like Yb fiber laser, is safe and compact than gas-made lasers (Olsen and Alting 1995; Powell 1998; Hernandez *et al.* 2007; Hernandez-Castaneda *et al.* 2009; Hernandez-Castaneda *et al.* 2011a; Hernandez-Castaneda *et al.* 2011b). Besides, structurally and practically, there is no need to use noxious gases, and the machining process does not release toxic gases dangerous to users nor ecologically harmful. Pulsed Nd: YAG laser is eco-friendly suited for cutting the black walnut veneer. Additionally, the Nd: YAG laser processes faster, cleaner, with less emission of hazardous smokes (Tahir *et al.* 2012a; Sharma and Yadava 2018). The Q-switching Nd: YAG laser has higher peak power leading to a clean, smooth cut due to its remarkable vaporization temperature (Kalokasidis *et al.* 2013).

The present study was limited in terms of process free of burrs and burning effect due to thermal deformation causing carbonization of black walnut veneer cut surface—these issues due to the complexity of the process parameters. For correction purposes and

efficient applicability, the right selection of nozzle and the energy carriage can lead to remarkable laser machining results. For micro-thin wood applications, Nd: YAG laser energy carried via an optical fiber wire can be gas-assisted (Tahir *et al.* 2012b; Li Jinzhe 2016; Jiang *et al.* 2016) or water-jet assisted (Yang *et al.* 2018), which provide excellent results, safety, and flexibility in the work environment. The use of Nd: YAG lasers is not solely eco-friendly but also guarantees the user's safety.

Further research related to the present study includes comparative and parametrical analyses of gas or water-assisted YAG laser cutting of micro-thin wood (veneers).

CONCLUSIONS

1. This study beneficially uses numerical methods to define and predict influenced parameters in cutting kerf width of black walnut veneer. In terms of cut surface quality, the laser cutting speed and output power show significant effects. For a selected laser output power condition, the kerf width increases while the laser cutting speed decreases and inversely.
2. Pulsed low powered Nd: YAG laser cut the black walnut veneer of 0.3 mm of thickness with minimum material thermal deformation, no significant burning effect, and a fast process with fewer restrictions.
3. Nd: YAG is a versatile laser suitable for cutting black walnut wood veneer, leading to a clean-cut result, smooth surface with narrow cut kerf. Plus, there is no limitation related to beam conductivity and reflection.
4. As a solid-state laser, Nd: YAG laser does not produce harmful gases. It is flexible, compact than the gas made lasers, safe, and eco-friendly.

ACKNOWLEDGMENTS

The authors thank the Forest and Woodworking Machinery Tech. Center of the Northeast Forestry University for the machine facilities under this research and all the work teams. Our gratitude goes to Northeast Forestry University and all members of the College of Mechanical and Electrical Engineering. Special thanks to the reviewers and co-authors for their valuable comments and suggestions.

Research Funding

This study was supported by the Applied Technology Research and Development Project in Heilongjiang Province of China (No. GA19A402); and Fundamental Research Funds for the Central Universities (No.2572020DR12).

REFERENCES CITED

- Almeida, J., Liang, D., and Vistas, C. R. (2018). "A doughnut-shaped Nd : YAG solar laser beam," *Optics and Laser Technology*, Elsevier Ltd, 106, 1-6. DOI: 10.1016/j.optlastec.2018.03.029
- Borges, B. M. F. D. C. A. (2008). "Laser cladding using filler powder and wire," Superior University of Lisbon.
- Chien, C. Y., and Gupta, M. C. (2005). "Pulse width effect in ultrafast laser processing of materials," *Applied Physics A: Materials Science and Processing*, 81(6), 1257-1263. DOI: 10.1007/s00339-004-2989-z
- Choudhury, I. A., and Shirley, S. (2010). "Laser cutting of polymeric materials: An experimental investigation," *Optics & Laser Technology* 42(3), 503-508. DOI: 10.1016/J.OPTLASTEC.2009.09.006
- Fork, R. L., Schehrer, K. L., Hirlimann, C., Avramopoulos, H., Fragnito, H. L., and Becker, P. C. (1989). "Amplification of femtosecond optical pulses using a double confocal resonator," *Optics Letters*, 14(19), 1068-10700. DOI: 10.1364/ol.14.001068
- Gautam, G. D., and Pandey, A. K. (2018). "Pulsed Nd:YAG laser beam drilling: A review," *Optics and Laser Technology* 100, 183-215. DOI: 10.1016/j.optlastec.2017.09.054
- Gong, Y. (2014). An on-line learning and training tool for laser cutting, Master's Thesis, University of Manchester, Manchester, United Kingdom.
- Guillas, C., Le, C., Theveney, S., and Lefebvre, P. (1990). "Comparative performances of CO₂ and YAG lasers in the cutting of stainless steel," *SPIE* 1277, 244-255.
- Hernandez-Castaneda, J. C., Kursad Sezer, H., and Li, L. (2011a). "The effect of moisture content in fibre laser cutting of pine wood," *Optics and Lasers in Engineering* 49(9-10), 1139-1152. DOI: 10.1016/j.optlaseng.2011.05.008
- Hernandez-Castaneda, J. C., Sezer, H. K., and Li, L. (2009). "Statistical analysis of ytterbium-doped fibre laser cutting of dry pine wood," *Proceedings of the Institution of Mechanical Engineers, Part B: Journal of Engineering Manufacture* 223(7), 775-789. DOI: 10.1243/09544054JEM1397
- Hernandez-Castaneda, J. C., Sezer, H. K., and Li, L. (2011b). "Single and dual gas jet effect in Ytterbium-doped fibre laser cutting of dry pine wood," *International Journal of Advanced Manufacturing Technology* 56(5-8), 539-552. DOI: 10.1007/s00170-011-3209-6
- Hernandez, J. C., Crouse, P., and Li, L. (2007). "High-power Yb-doped fibre laser for cutting dry pine wood," in: *World Congress on Engineering*, London, U.K., 2-7.
- Kalokasidis, K., Onder, M., Trakatelli, M. G., Richert, B., and Fritz, K. (2013). "The effect of Q-Switched Nd:YAG 1064 nm/532 nm laser in the treatment of onychomycosis in vivo," *Dermatology Research and Practice*, 2013. DOI: 10.1155/2013/379725
- Leone, C., Pagano, N., Lopresto, V., and Iorio, I. De. (2009). "Solid state Nd:YAG laser cutting of CFRP sheet: Influence of process parameters on kerf geometry and HAZ," in: *The 17th International Conference on Composite Materials*, 1-10.
- Li, J.-Z. (2016). *Microscopic Analysis and Experimental Study of Laser Processing Quality of Wood*, Master's Thesis, Northeast Forestry University, Harbin, China.
- Maiman, T. . (1960). "Stimulated optical radiation in ruby," *Nature Materials*, 187(4736), 493-494. DOI: 10.1038/187493a0
- Olsen, F. O., and Alting, L. (1995). "Pulsed laser materials processing, ND-YAG versus

- CO₂ lasers,” *CIRP Annals - Manufacturing Technology* 44(1), 141-145. DOI: 10.1016/S0007-8506(07)62293-8
- Peters, C. C., and Marshall, H. L. (1975). “Cutting wood materials by laser,” *US For Prod Lab Res Pap*, Juneau, Alaska 99801, 12.
- Pocorni, J., Han, S. W., Cheon, J., Na, S. J., Kaplan, A. F. H., and Bang, H. S. (2017). “Numerical simulation of laser ablation driven melt waves,” *Journal of Manufacturing Processes* 30, 303-312. DOI: 10.1016/j.jmapro.2017.09.032
- Powell, J. (1998). *CO₂ Laser Cutting*, Springer-Verlag London Limited. DOI: 10.1007/978-1-4471-1279-2
- Powell, J., and Kaplan, A. (2004). “Laser cutting: From first principles to the state of the art,” in: Pacific International Conference on Applications of Lasers and Optics, Laser Institute of America, Melbourne Australia, 1-6. DOI: 10.2351/1.5056075
- Schuoeker, D. (1989). “Laser cutting,” *Materials and Manufacturing Processes* 4(3), 311-330. DOI: 10.1080/10426918908956297
- Senthilkumar, V., Raja, P. P. K., Raj, R. P., Periyasamy, S. R., and Sakthidharan, S. (2016). “Experimental investigation and analysis of process parameters for laser cutting process,” *International Journal of Innovative Research in Science, Engineering and Technology*, 5(8), 151-158.
- Shabbusharma. (2020). “ND YAG laser working, construction and definition,” <<https://physicswave.com/>>.
- Sharma, A., and Yadava, V. (2013). “Modelling and optimization of cut quality during pulsed Nd:YAG laser cutting of thin Al-alloy sheet for curved profile,” *Optics and Lasers in Engineering*. DOI: 10.1016/j.optlaseng.2012.07.012
- Sharma, A., and Yadava, V. (2018). “Experimental analysis of Nd-YAG laser cutting of sheet materials - A review,” *Optics and Laser Technology* 98, 264-280. DOI: 10.1016/j.optlastec.2017.08.002
- Svelto, O. (2010). *Principles of Lasers, Persepsi Masyarakat Terhadap Perawatan Ortodontik Yang Dilakukan Oleh Pihak Non Profesional*, (D. C. Hanna, ed.), Springer London, Milan, Italy. DOI: 10.1007/978-1-4419-1302-9
- Tahir, B. A., Ahmed, R., Ashiq, M. G. B., Ahmed, A., and Saeed, M. A. (2012a). “Cutting of nonmetallic materials using Nd:YAG laser beam,” *Chinese Physics B*, 21(4), 44201. DOI: 10.1088/1674-1056/21/4/044201
- Tahir, B. A., Ahmed, R., Ashiq, M. G. B., Ahmed, A., and Saeed, M. A. (2012b). “Cutting of nonmetallic materials using Nd:YAG laser beam,” *Chinese Physics B*, 21(4). DOI: 10.1088/1674-1056/21/4/044201
- Trumpf. (2007). *Technical Information Laser Processing: CO₂ Laser*, SCRIBD.
- Wandera, C. (2006). *Laser Cutting of Austenitic Stainless Steel with a High Quality Laser Beam*, Master’s Thesis, Lappeenranta University of Technology, Lappeenranta, Finland.
- Xie, X.-Z., Xin, W., and Wei, H. (2008). “Theoretical model of CO₂ laser cutting non-metal material,” *Tool Engineering* 42(5), 19-21. DOI: 10.3969/j.issn.1000-7008.2008.05.006
- Jiang, X., Li, J., Bai, Y., Wu, Z., Yang, C., and Ma, Y. (2016). “Laser Cutting Wood Test and Influencing Factors of Processing Quality,” *Laser & Optoelectronics Progress*, 53(3), 031403. DOI: 10.3788/lop53.031403
- Yang, C., Deng, Z., Li, F., Jiang, X., Guo, C., and Ma, Y. (2018). “Design and experiment for a numerical control nanosecond water-jet-guided laser processing test bench,” *BioResources* 13(2017), 6098-6109. DOI: 10.15376/biores.13.3.6098-6109

- Yang, C., Jiang, T., Yu, Y., Dun, G., Ma, Y., and Liu, J. (2018). "Study on surface quality of wood processed by water-jet assisted nanosecond laser," *BioResources*, 13(2), 3125-3134. DOI: 10.15376/biores.13.2.3125-3134
- Yang, C., Liu, Q., Li, X., Miao, Q., Ma, Y., Doumbia, B., and Ren, C. (2019). "Theoretical process parameter calculation and test verification of laser cutting veneer," *Linye Kexue/Scientia Silvae Sinicae*, 55(12). DOI: 10.11707/j.1001-7488.20191218
- Yang, C., Lu, Y., Ma, Y., Ren, C., Bai, Y., and Cao, F. (2017). "Theoretical and experimental study on the cutting of wood by nanosecond pulse laser," *Linye Kexue/Scientia Silvae Sinicae*, 53(9), 151-156. DOI: 10.11707/j.1001-7488.20170918
- Zhou, B. H., and Mahdavian, S. M. (2004). "Experimental and theoretical analyses of cutting nonmetallic materials by low power CO₂-laser," *Journal of Materials Processing Technology* 146(2), 188-192. DOI: 10.1016/j.jmatprotec.2003.10.017
- Zhu, M., and Hall, J. L. (1997). *Atomic, Molecular, and Optical Physics: Electromagnetic Radiation, Experimental Methods in the Physical Sciences*.

Article submitted: November 10, 2020; Peer review completed: January 2, 2021;
Revisions accepted: February 1, 2021; Published: February 8, 2021.
DOI: 10.15376/biores.16.2.2416-2432